An Electron Spin Echo Envelope Modulation (ESEEM) Study of Electron–Nuclear Hyperfine and Nuclear Quadrupole Interactions of d_{z^2} Ground State Copper(II) Complexes with Substituted Imidazoles[1]

Feng Jiang,*,† Kenneth D. Karlin,‡ and Jack Peisach†

Department of Molecular Pharmacology, Albert Einstein College of Medicine, Yeshiva University, Bronx, New York 10461, and Department of Chemistry, The Johns Hopkins University, Baltimore, Maryland 21218

Received November 6, 1992

Electron spin echo envelope modulation (ESEEM) spectroscopy and angle-selective spectral simulation were used to study the electron–nuclear hyperfine and nuclear quadrupole interactions of substituted imidazoles axially coordinated in d_{z^2} ground state complexes with copper(II) tris(2-pyridylmethyl)amine (TMPA). Similar to the case of substituted imidazoles equatorially coordinated in $d_{x^2-y^2}$ ground state complexes with Cu^{II}(dien) (Jiang et al. *J. Am. Chem. Soc.* **1990**, *112*, 9035), it is the remote nitrogen that gives rise to modulations. The change of electronic structure of Cu(II) from a $d_{x^2-y^2}$ to a d_{z^2} ground state increases the electron–nuclear coupling for that nitrogen in imidazole by about 10%, while the nuclear quadrupole interaction is almost unaffected. For some substituted imidazoles, the weakening of ligand binding through steric interference not only reduces electron–nuclear coupling but also changes the nuclear quadrupole interaction. Alteration of the strength of the hydrogen bond at the remote nitrogen can be recognized from changes in the nuclear quadrupole parameters.

Various Cu(II) model complexes have been used to mimic the active-site structures of Cu(II) proteins, on the basis of their similarities in specific structural features, in spectroscopic features, or both.[2-8] As many binding sites in copper proteins have irregular geometries, structural modeling becomes difficult while spectroscopic modeling may not always give a reliable indication of the actual structure in the protein. In every case thus far examined, the binding sites of all Cu(II) proteins contribute nitrogenous ligands to the metal ion.[9,10] For this reason, intensive investigations have been carried out on models containing nitrogen ligands as a means of understanding the chemistry of Cu(II) coordinated to proteins.

Most Cu(II) complexes with nitrogen ligands tend to have an elongated octahedral or square pyramidal coordination geometry, with four close-lying ligands in a nearly planar array.[11a] This geometric arrangement is indicative of a $d_{x^2-y^2}$ ground state complex whose EPR spectrum is characterized by $g_\perp < g_\parallel$.[12] In proteins as well as in models, various constraints may be imposed on the metal–ligand structure so that the four close-lying ligands no longer encompass a plane, leading to a tetrahedral distortion. This is accompanied by a reduction in the EPR parameters $A_\parallel$ and $g_\parallel$.[9b]

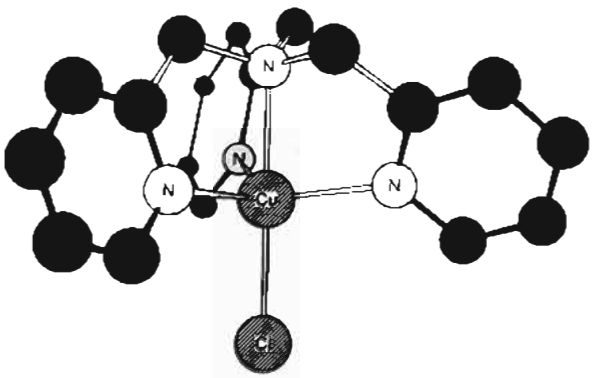

Figure 1. Chem 3D drawing of $[Cu^{II}(TMPA)(Cl)]^+$, which has trigonal bipyramidal coordination geometry. Relevant bond lengths (Å) and angles (deg): Cu–N(1), 2.050; Cu–N(2), 2.062; Cu–N(3), 2.060; Cu–N(4), 2.072; Cu–Cl, 2.233; N(1)–Cu–N(2), 81.5; N(1)–Cu–N(3), 81.1; N(1)–Cu–N(4), 80.8; N(1)–Cu–Cl, 179.1; N(2)–Cu–N(3), 118.2; N(2)–Cu–N(4), 118.8; N(2)–Cu–Cl, 97.6; N(3)–Cu–N(4), 116.0; N(3)–Cu–Cl, 99.6; N(4)–Cu–Cl, 99.4.

Another type of distortion of a Cu(II) site is brought about when the model ion is forced into a trigonal bipyramidal coordination geometry by binding to a tripodal tetradentate ligand.[2] A case in point is the Cu(II) complex formed with tris(2-pyridylmethyl)amine, TMPA. A fifth ligand, such as Cl^-, F^-, or imidazole, can be added trans to the amine nitrogen to the polydentate ligand (Figure 1).[3] The structural constraints due to the chelate ring size cause the axial amine nitrogen to lie close to Cu(II) (~2.05 Å, as compared to ~2.25 Å for the axial nitrogen in a square pyramidal Cu(II) complex).[2,3] The energy of the d_{z^2}

* To whom correspondence should be addressed.
† Yeshiva University.
‡ The Johns Hopkins University.

(1) Abbreviations: ESEEM, electron spin echo envelope modulation; TBP, trigonal bipyramidal; TMPA, tris(2-pyridylmethyl)amine; CW, continuous wave; EFG, electric field gradient; ENDOR, electron–nuclear double resonance.

(2) Zubieta, J.; Karlin, K. D.; Hayes, J. C. In *Copper Coordination Chemistry: Biochemical & Inorganic Perspectives*; Karlin, K. D., Zubieta, J., Eds.; Adenine Press: New York, 1982; pp 97–108.
(3) Karlin, K. D.; Hayes, J. C.; Juen, S.; Hutchinson, J. P.; Zubieta, J. *Inorg. Chem.* **1982**, *21*, 4106.
(4) (a) Bencini, A.; Bertini, I.; Gatteschi, D.; Scozzafava, A. *Inorg. Chem.* **1978**, *17*, 3194. (b) Seffen, G.; Reinen, D.; Stratemeier, H.; Riley, M. J.; Hitchman, M. A.; Matthies, H. E.; Recker, K.; Wallrafen, F.; Niklas, J. R. *Inorg. Chem.* **1990**, *29*, 2123. (c) Giordano, R. S.; Bereman, R. D. *J. Am. Chem. Soc.* **1974**, *96*, 1019.
(5) Goldfarb, D.; Fauth, J.-M.; Tor, Y.; Shanzer, A. *J. Am. Chem. Soc.* **1991**, *113*, 1941.
(6) Mims, W. B.; Peisach, J. *J. Chem. Phys.* **1978**, *19*, 4921.
(7) Jiang, F.; McCracken, J.; Peisach, J. *J. Am. Chem. Soc.* **1990**, *112*, 9035.
(8) Colaneri, M.; Peisach, J. *J. Am. Chem. Soc.* **1992**, *114*, 5335.
(9) (a) McMillin, D. R.; Engeseth, H. R. In *Biological & Inorganic Copper Chemistry*; Karlin, K. D., Zubieta, J., Eds.; Adenine Press: New York, 1984; Vol. I, pp 1–10. (b) Rydén, L. In *Copper Proteins and Copper Enzymes*; Lontie, R., Ed.; CRC Press: Boca Raton, FL, 1984; Vol. I, pp 158–183.
(10) *Copper Proteins*; Spiro, T. G., Ed.; Wiley-Interscience: New York, 1981.
(11) (a) Cotton, F. A.; Wilkinson, G. *Advanced Inorganic Chemistry*, 5th ed.; Wiley-Interscience: New York, 1988; pp 766–774. (b) Cotton, F. A.; Wilkinson, G. *Advanced Inorganic Chemistry*, 4th ed.; Wiley-Interscience: New York, 1980; pp 638–652.
(12) Abragam, A.; Bleaney, B. *Electron paramagnetic resonance of transition ions*; Clarendon Press: Oxford, U.K., 1970; pp 455–469.

0020-1669/93/1332-2576$04.00/0

orbital which is involved in bonding of the trans axial ligands is raised so that the unpaired electron resides mostly in this orbital.[11b] Characteristic of this type of geometric organization is an EPR spectrum with $g_\parallel < g_\perp$.[12,13] The spectra of the Cu_B site in cytochrome *c* oxidase and the partially reduced type 3 copper center of tree laccase[14] resemble those with a reversal of $g_\parallel$ and $g_\perp$ from that normally seen for $d_{x^2-y^2}$ ground state complexes.

ESEEM spectroscopy, a pulsed EPR technique, has been applied to the study of metal binding sites in various Cu(II) proteins.[15-18] Investigations of $d_{x^2-y^2}$ ground state Cu(II) model complexes containing imidazole or substituted imidazole[6,7] have aided in the interpretation of protein data. For Cu^{II}(dien)-(substituted imidazole) models, we showed that the differences in quadrupole parameters of the remote ^{14}N of coordinated histidine imidazole in Cu(II) proteins could be attributed to variations in hydrogen bonding at this nitrogen.[7] In the present investigation, we have extended our ESEEM studies to imidazole and substituted imidazoles axially coordinated to Cu(II) in d_{z^2} ground state complexes and determined the electron–nuclear coupling parameters by angle-selective ESEEM simulations. We show that the change of coordination geometry from square planar to trigonal bipyramidal and the concomitant change of the electronic configuration from a $d_{x^2-y^2}$ to a d_{z^2} ground state result in a small increase of the electron–nuclear coupling but have little effect on the nuclear quadrupole parameters. Similarly, we show that altering the strength of hydrogen bonding of an axially coordinated imidazole gives rise to differences in the ESEEM spectrum comparable to those observed in $d_{x^2-y^2}$ complexes.

Experimental Section

Sample Preparation. $[Cu^{II}(TMPA)(H_2O)](ClO_4)_2$[19] dissolved in either H_2O or acetone to a final concentration of 4 mM was titrated with imidazole, 1-methylimidazole, 2-methylimidazole, 4-methylimidazole, or 1,2-dimethylimidazole, using continuous-wave EPR. For those prepared in H_2O, the pH was maintained at 7.5–7.6 before an equal volume of ethylene glycol was added to ensure good glass formation required for low-temperature EPR studies. Due to differences in pK_a and affinity, the concentrations of substituted imidazoles needed to form paramagnetically pure complexes in aqueous samples varied. The ratios of Cu^{II}-(TMPA) to substituted imidazoles required to form paramagnetically pure species are given in Table I. For samples prepared in acetone, a stoichiometric equivalent of substituted imidazole was sufficient. Here, an equal volume of toluene was added for good glass formation. Samples of Cu^{II}(dien)(substituted imidazole) models were prepared as previously.[7]

EPR Spectroscopy. X-band continuous-wave EPR spectra were obtained at 77 K with a Varian E112 spectrometer, equipped with a Varian NMR gaussmeter and a Systron Donner frequency counter.

Table I. Compositions and EPR Parameters for $[Cu^{II}(TMPA)(substituted\ imidazole)](ClO_4)_2$ Complexes Prepared in H_2O/Ethylene Glycol

Cu^{II}(TMPA) complex with	Cu:ligand	$g_\parallel$[a]	$A_\parallel$[b] (MHz)	$g_\perp$[c]	$A_\perp$ (MHz)
H_2O		2.0	192	2.199	319
imid	1:4	~2.0	220	2.199	370
1-CH_3-imid	1:5	~2.0	220	2.199	370
4-CH_3-imid	1:1	~2.0	220	2.199	370
2-CH_3-imid	1:100	~2.0	220	2.208	390
1,2-$(CH_3)_2$-imid	1:100	~2.0	220	2.208	390

[a] The lack of hyperfine splitting in the parallel region of the spectrum prevented an accurate determination of $g_\parallel$ and $A_\parallel$. [b] The uncertainty in the determination of the hyperfine coupling is 20 MHz. [c] The uncertainty in $g_\perp$ is 0.002.

Spectral simulations were carried out by a method described previously.[20] The spectrum characterized by $g_\parallel < g_\perp$ was used to check the formation of d_{z^2} ground state complex as well as the paramagnetic purity of each sample.

ESEEM were obtained with a home-built pulsed EPR spectrometer,[17c] equipped with a folded strip-line cavity[21] which accommodated 4 mM quartz EPR tubes. Data were collected using a stimulated echo (90°–τ–90°–T–90°) pulse sequence.[22] The value of τ, the spacing between the first and second microwave pulses, was set to multiples of the proton Zeeman frequency harmonics so that modulations due to weakly coupled protons were largely suppressed.[22] ESEEM spectra were obtained by Fourier transformation using a modified version of the dead-time reconstruction method of Mims.[23] Typical measurement conditions were the following: microwave frequency, 8.8 GHz; microwave power, 45 W; pulse width, 20 ns; sample temperature, 4.2 K; pulse repetition rate, 100 Hz.

ESEEM Spectral Simulations. ESEEM spectral simulations were achieved by using the density matrix formalism of Mims,[24] together with an angle-selection averaging scheme originally developed for field-dependent ENDOR.[25] Under favorable conditions, the electron–nuclear coupling tensor and nuclear quadrupole tensor can be obtained by spectral simulation for spectra collected at several different magnetic field settings across the EPR absorption in an angle-selection procedure.[27] Nine parameters are used to describe these two tensors. e^2qQ and η describe the magnitude and the symmetry of the quadrupole tensor; the three principal values are $e^2qQ(1-\eta)/2$, $e^2qQ(1+\eta)/2$, and e^2qQ. Euler angles, α, β, and γ, describe rotations needed to align the principal axes of the quadrupole tensor with those of the **g** tensor. The electron–nuclear coupling tensor is taken to be axial. The three principal values are $A_{iso} - F$, $A_{iso} - F$, and $A_{iso} + 2F$, where A_{iso} is the isotropic component and F, the anisotropic component. Assuming a point dipole–dipole interaction the unpaired electron and the coupled nucleus over an effective distance, r_{eff}, $F = g_e\beta_e g_N\beta_N/r_{eff}^3$. Here, g_e and g_N are the electron and the nuclear g factor, and β_e and β_N are the Bohr magnetron and the nuclear magneton. Due to the axial nature of the electron–nuclear coupling tensor, two angles θ_N and ϕ_N, which specify the apparent spherical polar coordinates of the interacting nucleus, are sufficient to describe the orientation of the principal axes of this tensor relative to those of the **g** tensor.

^{14}N Modulation. In the presence of an external magnetic field, ^{14}N experiences three kinds of interactions: the nuclear Zeeman interaction,

(13) (a) Kokoszka, G.; Karlin, K. D.; Padula, F.; Baranowski, J.; Goldstein, C. *Inorg. Chem.* **1984**, *23*, 4378. (b) Barbucci, R.; Bencini, A.; Gatteschi, D. *Inorg. Chem.* **1977**, *16*, 2117. (c) Addison, A. W.; Hendriks, H. M. J.; Reedijk, J.; Thompson, L. K. *Inorg. Chem.* **1981**, *20*, 103.

(14) (a) Reinhammar, B.; Malkin, R.; Jensen, P.; Karlsson, B.; Andreasson, L.-E.; Assa, R.; Vanngard, T.; Malmstrom, B. G. *J. Biol. Chem.* **1980**, *11*, 5000. (b) Reinhammar, B. J. *Inorg. Biochem.* **1983**, *18*, 113. (c) Cline, J.; Reinhammar, B.; Jensen, P.; Venters, R.; Hoffman, B. M. *J. Biol. Chem.* **1983**, *258*, 5124.

(15) (a) Mims, W. B.; Peisach, J. *J. Biol. Chem.* **1979**, *254*, 4321. (b) Kosman, D. J.; Peisach, J.; Mims, W. B. *Biochemistry* **1980**, *19*, 1304. (c) Zweier, J. L.; Peisach, J.; Mims, W. B. *J. Biol. Chem.* **1982**, *257*, 10314.

(16) McCracken, J.; Desai, P. R.; Papadopoulos, N. J.; Villafranca, J. J.; Peisach, J. *Biochemistry* **1988**, *27*, 4133.

(17) (a) Mondovi, B.; Morpurgo, L.; Agostinelli, E.; Befani, O.; McCracken, J.; Peisach, J. *Eur. J. Biochem.* **1987**, *168*, 503. (b) McCracken, J.; Pember, S.; Benkovic, S. J.; Villafranca, J. J.; Miller, R. J.; Peisach, J. *J. Am. Chem. Soc.* **1988**, *110*, 1069. (c) McCracken, J.; Peisach, J.; Dooley, D. M. *J. Am. Chem. Soc.* **1987**, *109*, 4064.

(18) (a) Mondovi, B.; Graziani, M. T.; Mims, W. B.; Oltzik, R.; Peisach, J. *Biochemistry* **1977**, *16*, 4198. (b) Avigliano, L.; Davis, J. L.; Graziani, M. T.; Marchesini, A.; Mims, W. B.; Mondovi, B.; Peisach, J. *FEBS Lett.* **1981**, *136*, 80. (c) Fee, J. A.; Peisach, J.; Mims, W. B. *J. Biol. Chem.* **1981**, *256*, 1910.

(19) Jacobson, R. R.; Tyeklár, Z.; Karlin, K.; Zubieta, J. *Inorg. Chem.* **1991**, *30*, 2035.

(20) (a) Nilges, M. J. Ph.D. Thesis, University of Illinois, Urbana, IL, 1979. (b) Belford, R. L.; Nilges, M. J. Presented at the International Electron Paramagnetic Resonance Symposium, 21st Rocky Mountain Conference, Denver, CO, 1979. (c) Maurice, A. M. Ph.D. Thesis, University of Illinois, Urbana, IL, 1981.

(21) Britt, R. D.; Klein, M. P. *J. Magn. Reson.* **1987**, *74*, 535.

(22) Mims, W. B.; Peisach, J. In *Biological Magnetic Resonance*; Berliner, L. J., Reuben, J., Eds.; Plenum Press: New York, 1981; Vol. 3, pp 213–263.

(23) Mims, W. B. *J. Magn. Reson.* **1984**, *59*, 291.

(24) Mims, W. B. *Phys. Rev.* **1972**, *5*, 2409.

(25) (a) Hurst, G. C.; Henderson, T. A.; Kreilick, R. W. *J. Am. Chem. Soc.* **1985**, *107*, 7294. (b) Henderson, T. A.; Hurst, G. C.; Kreilick, R. W. *J. Am. Chem. Soc.* **1985**, *107*, 7299.

(26) Flanagan, K. L.; Singel, D. J. *J. Chem. Phys.* **1987**, *87*, 5606.

(27) (a) Cornelius, J. B.; McCracken, J.; Clarkson, R.; Belford, R. L.; Peisach, J. *J. Phys. Chem.* **1990**, *94*, 6977. (b) McCracken, J.; Cornelius, J. B.; Peisach, J. In *Pulsed EPR: A New Field of Applications*; Keijzers, C. P., Reijerse, E. J., Schmidt, J., Eds.; North Holland: Amsterdam, 1989; pp 156–161.

the electron–nuclear hyperfine coupling, and the nuclear quadrupole interaction. It has been shown that nitrogen modulations are best observed when the nuclear Zeeman interaction is comparable to the electron–nuclear interaction,[6] termed the condition of "exact cancellation".[26] As a result, for one of the electron spin manifolds, the nuclear Zeeman interaction and the electron–nuclear interaction cancel each other so that the nuclear quadrupole interaction essentially determines the energy levels. This gives rise to three sharp lines in the ESEEM spectrum whose frequencies ν_0, ν_-, and ν_+, are related to e^2qQ, the quadrupole coupling constant, and η, the asymmetry parameter.

$$\nu_\pm = {}^3/_4 e^2qQ(1 \pm \eta/3) \quad (1)$$

$$\nu_0 = {}^1/_2 e^2qQ\eta \quad (2)$$

Euler angles as well as the electron–nuclear coupling parameters determine the relative intensities of these three sharp lines.

For the other spin manifold, the nuclear Zeeman interaction and the electron–nuclear coupling are additive. Due to the anisotropy of the electron–nuclear coupling and the averaging effect of the frozen-solution sample (rather than a single crystal), a broad line representing a $\Delta M_I = 2$ transition at a frequency about twice the electron–nuclear coupling is observed. The shape and frequency of this double quantum line are determined by A_{iso} and r_{eff}, as well as θ_N, ϕ_N, α, β, and γ.

Under the condition of "exact cancellation", the frequencies of the low-frequency quadrupole lines are used to obtain e^2qQ and η (eqs 1 and 2). The intensities are, however, not sufficient to uniquely determine Euler angles α, β, and γ. Only when there is a large field dependence in both the intensity and the frequency of the quadrupole and the double-quantum lines (i.e. away from the "exact cancellation" condition), can α, β, and γ be determined by spectral simulation.[27a,28] For Cu^{II}(TMPA)(substituted imidazole) complexes studied at X-band, the field dependence is not sufficiently large to make this determination (see below). However, if we know the structure of a Cu^{II}(TMPA)(substituted imidazole) complex and assume that the principal direction of the g tensor is aligned with the symmetry axis, then the Euler angles, α, β, and γ, as well as the azimuthal, and polar angles, θ_N and ϕ_N, can be estimated.

Using the values for these five angles estimated as described above, A_{iso} and r_{eff} can be obtained from fitting the double-quantum line in spectral simulations at different magnetic fields.

Results and Discussion

d_{z^2} Ground State Copper(II) Complexes. The tripodal tetradentate ligand TMPA forms a TBP complex with Cu(II). X-ray crystallographic studies[3,19] of $[Cu^{II}(TMPA)(Cl)]PF_6$ and $[Cu^{II}(TMPA)(F)]PF_6$ show that Cl^- or F^- and the aliphatic amine nitrogen occupy two axial positions, while the three pyridyl nitrogens encompass an equatorial plane (Figure 1). Regardless of the difference in the exogenous axial ligand, each of the in-plane bond angles are close to 120° and the three Cu–N in-plane bond lengths are nearly equal, as expected for an ideal TBP geometry. The difference between Cl^- and F^- results in small differences in the axial bond length and bond angles, having little effect on the overall coordination geometry. The EPR spectra for both complexes, like other Cu(II) complexes with TBP coordination,[13] have $g_\parallel < g_\perp$, suggesting that the unpaired electron of Cu(II) resides mainly in a d_{z^2} orbital.

Although no X-ray structural study has been carried out for $[Cu^{II}(TMPA)(H_2O)](ClO_4)_2$ or for any of the substituted imidazole complexes, their EPR spectra in frozen solution suggest TBP coordination as well (Figure 2a). All Cu^{II}(TMPA)(substituted imidazole) complexes studied here, like the parent compound, have a characteristic d_{z^2} ground state Cu(II) CW EPR spectrum. The spectrum of the imidazole complex (Figure 2b) is the same as that of the 1-methylimidazole complex, suggesting identical ligand atom composition and inner-sphere coordination geometry (Table I).[29] The spectra of the 2-methylimidazole (Figure 2d) and 1,2-dimethylimidazole complexes

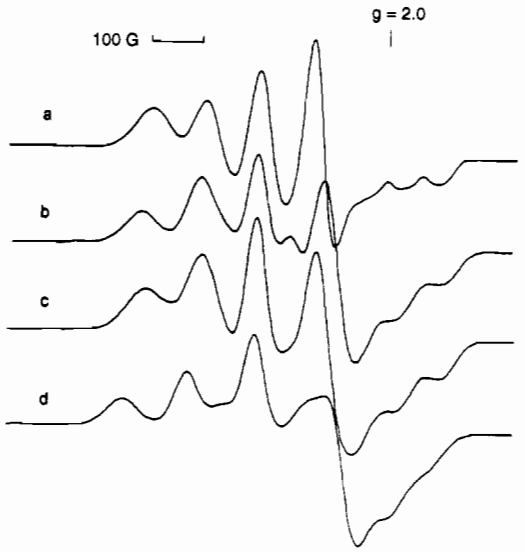

Figure 2. CW EPR spectra of aqueous samples of $[Cu^{II}(TMPA)(L)](ClO_4)_2$, with L = H_2O (a), imidazole (b), 4-methylimidazole (c), and 2-methylimidazole (d). Experimental conditions: microwave frequency, 9.09 GHz; microwave power, 5.0 mW; modulation amplitude, 5.0 G; sample temperature, 77 K.

are also alike but differ from those of the imidazole and 1-methylimidazole complexes, suggesting differences in ligand coordination geometry. Therefore, although the addition of a methyl group at the remote nitrogen of the axially coordinated imidazole has no effect on the geometry of the copper site, the addition of a methyl group at C(2) likely hinders its binding to Cu(II) (see below). This results in a reduction in ligand affinity and an increase in the coupling between the unpaired electron and the Cu(II) nucleus, as judged from an increase in $A_\perp$ (Table I).[30]

ESEEM Spectra of Substituted Imidazoles. For $Cu^{II}(TMPA)(H_2O)$, a spin echo is obtained, but no nitrogen modulations are seen. The coupling between the Cu(II) unpaired electron and directly coordinated pyridyl or amine nitrogen nuclei of TMPA is therefore either too large or too small to give rise to ESEEM at X-band.[6] Strong nitrogen modulations, however, are observed for all the Cu^{II}(TMPA)(substituted imidazole) complexes studied.

The coupling between the directly coordinated imidazole nitrogen and Cu(II), similar to that between Cu(II) and the amine nitrogen of TMPA, is inappropriate to give rise to envelope modulations.[6] Also, were the modulations to arise from the directly coordinated ^{14}N of both imidazole and 1-methylimidazole, little difference in ESEEM frequencies would be expected, as found for Mn^{2+} model complexes.[31] Since large differences comparable to those seen for corresponding $d_{x^2-y^2}$ ground state complexes were observed, it is the remote ^{14}N that gives rise to the ESEEM (Table II and Table II in ref 7).

ESEEM spectra were obtained at six different magnetic field settings across the EPR absorption for the Cu^{II}(TMPA)(substituted imidazole) complexes listed in Table II. Characteristic

(28) Jiang, F.; Conry, R. R.; Bubacco, L.; Tyeklár, Z.; Jacobson, R. R.; Karlin, K. D.; Peisach, J. Submitted for publication in *J. Am. Chem. Soc.*

(29) The EPR parameters were required for the simulation of the angle-selective ESEEM spectrum. The error in the determination of $g_\parallel$ has very little effect on the determination of the nuclear quadrupole parameters but does have an effect on the electron–nuclear coupling, and especially r_{eff}. However, this effect is smaller than that introduced by the uncertainty of other experimental parameters (e.g. the field width) in the ESEEM simulation.

(30) The d_{z^2} ground state $[Cu^{II}(TMPA)(substituted\ imidazole)](ClO_4)_2$ complexes break down to $d_{x^2-y^2}$ ground state complexes in the presence of large excess of ligand, as judged from changes in line shape of the EPR spectrum. In the samples used in ESEEM studies, less than 10% consisted of the parent $[Cu^{II}(TMPA)(H_2O)](ClO_4)_2$ complex or the $d_{x^2-y^2}$ ground state breakdown product.

(31) McCracken, J.; Peisach, J.; Bhattacharyya, L.; Brewer, F. *Biochemistry* **1991**, *30*, 4486.

Table II. ESEEM Frequencies and Simulation Parameters (MHz) for $[Cu^{II}(TMPA)(substituted\ imidazole)](ClO_4)_2$ Complexes

ligand	solvent[a]	ν_0	ν_+	ν_-	ν_d[b]	A_{iso}[c]	r_{eff} (Å)	e^2qQ	η
imid	aqueous	0.71	0.71	1.41	3.98	1.80	3.0	1.41	0.90
	acetone	0.63	0.73	1.35	4.01	1.80	3.0	1.41	0.83
4-CH_3-imid	aqueous	0.59	0.87	1.49	3.96	1.80	3.0	1.55	0.76
	acetone	0.71	0.71	1.44	3.98	1.80	3.0	1.50	0.85
2-CH_3-imid	aqueous	0.59	0.97	1.56	3.86 4.08	1.75	3.2	1.65	0.73
	acetone	0.76	0.76	1.50	3.93	1.75	3.2	1.58	0.87
1,2-$(CH_3)_2$-imid	aqueous	0.16	1.67	1.67	4.30	1.97	3.5	2.18	0.08
	acetone	<0.1	1.58	1.73	4.13 4.32	1.97	3.5	2.15	0.15
1-CH_3-imid	aqueous	<0.1	1.47	1.56	4.29	2.06	3.3	1.98	0.08
	acetone	<0.1	1.49	1.49	4.30	2.08	3.3	1.95	0.05

[a] Aqueous samples consist of a 1:1 water/ethylene glycol mixture. Samples in acetone are diluted 1:1 with toluene. [b] ν_d is the frequency of the broad double-quantum transition observed in the spectrum with the magnetic field set at 2981 G. In some cases, this spectral feature can be resolved into two lines. [c] The error in A_{iso} is 0.05 MHz and in r_{eff} is 0.2 Å.

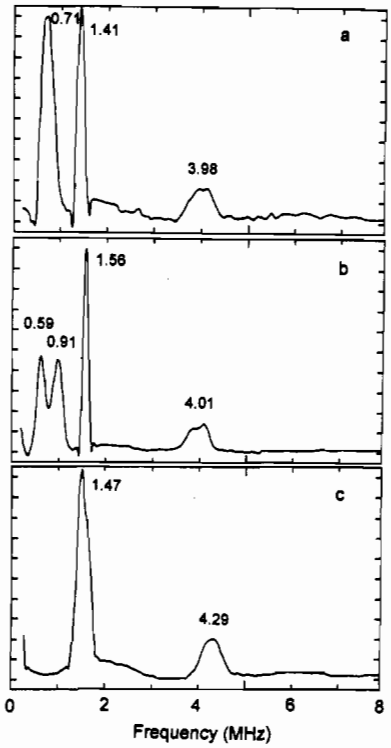

Figure 3. ESEEM spectra of $[Cu^{II}(TMPA)(L)](ClO_4)_2$ complexes in H_2O/ethylene glycol, with L = imidazole (a), 2-methylimidazole (b), and 1-methylimidazole (c). Measurement conditions: microwave frequency, 8.627 (a), 8.633 (b), and 8.626 GHz (c); magnetic field 2981 G; sample temperature, 4.2 K.

^{14}N ESEEM spectra were obtained for all of them. The intensities of the low-frequency quadrupole lines change with magnetic field, but the frequencies are almost field independent. The coupling between the Cu(II) unpaired electron and the remote nitrogen nucleus of the various substituted imidazoles coordinated to Cu^{II}(TMPA), therefore, satisfies the "exact cancellation" condition (Table II).

For aqueous samples of Cu^{II}(TMPA) with imidazole (Figure 3a), two of the three low-frequency quadrupole lines are so close to one another that they cannot be resolved; the spectrum has three rather than four lines. The asymmetry parameter η is 0.90. All three quadrupole lines are, however, well resolved in the spectrum for the complex with either 2-methylimidazole (Figure 3b) or 4-methylimidazole. Values for η are reduced, 0.73 for 2-methylimidazole and 0.76 for 4-methylimidazole. Only one quadrupole line is observed for the 1-methylimidazole complex (Figure 3c), because not only do the two high-frequency quadrupole lines coalesce into a single unresolved line but also the lowest quadrupole transition has a frequency below the resolution of the spectrometer and cannot be seen. The value for η is near zero.

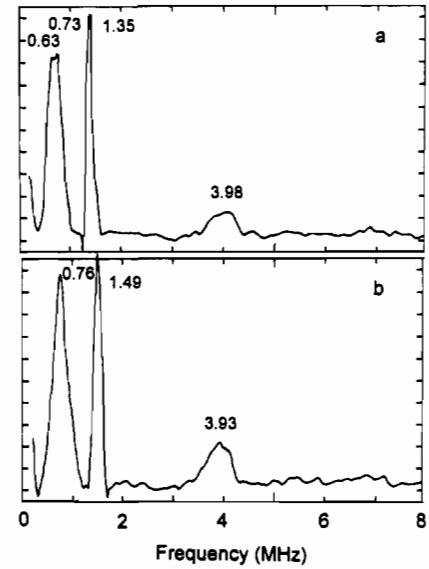

Figure 4. ESEEM spectra of $[Cu^{II}(TMPA)(imidazole)](ClO_4)_2$ (a) and $[Cu^{II}(TMPA)(2\text{-methylimidazole})](ClO_4)_2$ (b) in acetone/toluene. Measurement conditions: microwave frequency, 8.612 (a) and 8.560 GHz (b); magnetic field, 2981 G; sample temperature, 4.2 K.

The ESEEM spectra for 2-methylimidazole (Figure 4b) and 4-methylimidazole complexes (not shown) in acetone/toluene are significantly different from those in water/ethylene glycol, even though the CW EPR spectra show no change with solvent. The two well-resolved, low-frequency quadrupole lines ($\eta \sim 0.75$) observed in aqueous samples (Figure 3b) coalesce so that the ESEEM spectra become similar to that of the imidazole complex ($\eta \sim 0.9$). This suggests that the electric field gradient (EFG) giving rise to the nuclear quadrupole interaction at the remote nitrogen of 4-methylimidazole and 2-methylimidazole is changed by the action of solvent. A less dramatic change with solvent is seen, though, in the spectrum for the imidazole complex (Figure 4a), and almost no change is seen for the 1-methylimidazole and 1,2-dimethylimidazole complexes (Table II).

Spectral Simulations. At a particular magnetic field setting within the EPR absorption envelope, only a selected population of molecules having a particular orientation with respect to the magnetic field are in resonance. The composition of the population of molecules selected is dependent on the effective field width which, in turn, is determined by the pulse duration in the experiment. With the 20-ns microwave pulse employed in our studies, all molecules resonating within 35 G around the magnetic field setting are excited. The ESEEM spectrum may, therefore, be considered an average of single-crystal-like spectra of these molecules. For samples exhibiting large g and A anisotropies, there are fewer molecular orientations which fulfill the resonance condition at the ends of the EPR absorption than in the middle. Therefore, at the two ends of the EPR absorption, the ESEEM

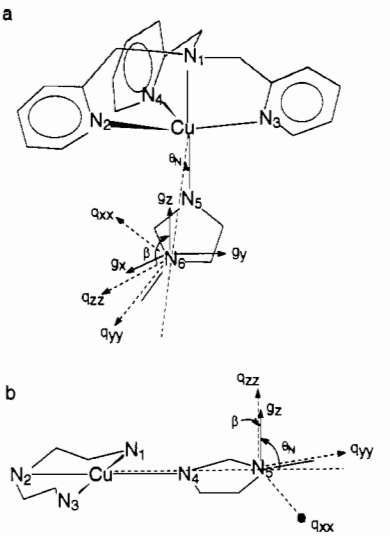

Figure 5. Schemtic drawing of $[Cu^{II}(TMPA)(1\text{-methylimidazole})](ClO_4)_2$ (a) and Cu^{II}(dien)(1-methylimidazole) (b) showing the principal-axis system of the **g** tensor and of the electric field gradient tensor (**q**) at the remote nitrogen of 1-methylimidazole. The direction of g_z is along the Cu(II)–N(1) bond (a) or perpendicular to the Cu(II)–dien plane (b); g_x and g_y are in any direction in the equatorial plane. The direction of q_{zz} is perpendicular to the imidazole plane, q_{yy} is along the N(6,5)–CH_3 bond, and q_{xx} is in-plane and perpendicular to the N(6,5)–CH_3 bond.

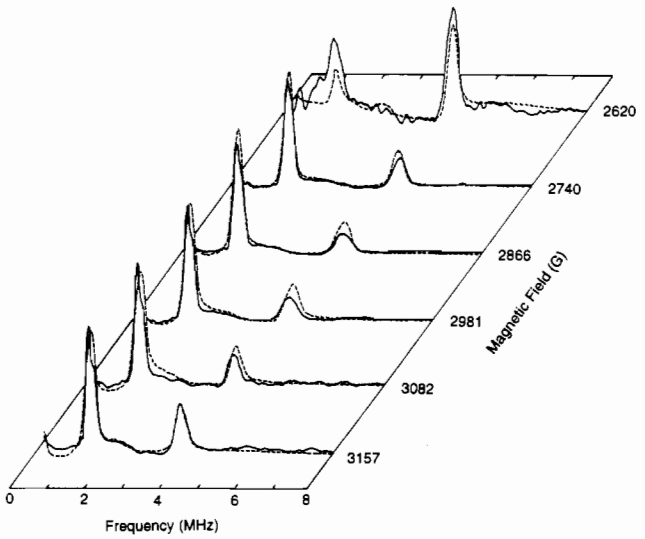

Figure 6. Three-pulse ESEEM spectra and spectral simulations for $[Cu^{II}(TMPA)(1\text{-methylimidazole})](ClO_4)_2$ at six different magnetic field settings within the EPR absorption: solid line, experimental data; dashed line, simulation. Measurement conditions: microwave frequency, 8.562 GHz; temperature, 4.2 K. The magnetic fields at which each spectrum was collected are indicated and the τ value for each spectrum is equal to twice the proton periodicity at each magnetic field. Simulation parameters are listed in Table II.

spectrum has more single-crystal-like character and the averaging effect is more sensitive to the field width ΔH.

The magnetic field width is one of the experimental parameters required for an ESEEM simulation. A simulation for the spectrum obtained in the middle of the EPR absorption, 3035 G, using a field width of 15 G, yields a split double-quantum line, which is not observed in the data. Better fits to the data are obtained when ΔH is increased to 30 G. A further increase, beyond 40 G, causes little change in the shape of the double-quantum transition in the simulated spectrum. However, this increase of ΔH from 15 G to more than 40 G results in changes in both the intensity and frequency of the double-quantum line in simulations for spectra obtained at the ends of EPR absorption, which is critical in the determination of r_{eff}. Because of the limit of instrumentation, the microwave pulse is not a perfect square wave and the field width might be actually larger than 35 G. Consistent with an earlier study,[7] 50 G was used in all simulations presented here. The use of 50 G as compared to 15 G in spectral simulation results in about a 4% difference in the determination of r_{eff}.

Determination of the Electron–Nuclear Coupling. The principal direction of the **g** tensor is correlated with the symmetry axis of the molecule. The X-ray structure of $[Cu^{II}(TMPA)(Cl)]PF_6$ shows that it has almost ideal TBP geometry (Figure 1). The N(1)–Cu(II)–Cl angle is 179.1°, showing that the amine nitrogen, Cu(II), and Cl^- are almost collinear. The three pyridyl nitrogens are disposed nearly symmetrically around this line. This nearly ideal C_3 geometry allows us to reasonably assume that g_z lies along the Cu–N(1) axis. Even though a rhombic **g** tensor might be expected for this complex, an apparent axial EPR spectrum was obtained due to the vibronic effects which average the two other **g** components.[13a] Therefore, g_x or g_y can be assumed to lie in any direction perpendicular to the g_z axis.

Even though there are no X-ray structures available for our model complexes with substituted imidazoles, we shall assume a structure similar to that of $[Cu^{II}(TMPA)(Cl)]PF_6$. We can also assume that the imino nitrogen of a substituted imidazole binds to Cu^{II}(TMPA) through its lone-pair orbital along the Cu(II)–N(1) direction (Figure 5) and that the Cu(II)–N(5) bond length is about 2.0 Å. The direction of Cu(II)–N(6) is then 9.3° away from Cu(II)–N(1), and this defines θ_N (Figure 5a).[32]

The principal directions of the quadrupole tensor, q_{xx}, q_{yy}, and q_{zz},[33] are correlated with the directions of the valence-shell orbitals of ^{14}N. Although there is an ambiguity in the direction of q_{zz} for the remote ^{14}N of imidazole,[7,34] the direction of q_{zz} for 1,2-dimethylimidazole, as determined by a single-crystal ESEEM study of Cu(II)-doped Zn^{II}(1,2-dimethylimidazole)$_2Cl_2$,[35] is perpendicular to the imidazole plane and q_{yy} lies along the N(1)–CH_3 bond. Because the EFG at the remote nitrogen of 1-methylimidazole is similar to that of 1,2-dimethylimidazole (both contain an *N*-methyl group rather than a proton),[7] the direction of q_{zz} should be similar for both (Figure 5a).[36] Then, α and β are 60 and 90°. Due to the axial symmetry of the **g** tensor, the assignment of the g_x and g_y axes are arbitrary. Therefore, a value of 0° was used for γ and ϕ_N in simulations. In support of the above assignment of the orientation of the quadrupole tensor, the best fits for both the frequency and line shape of the double-quantum transition were obtained using 90° for β and 10° for θ. We obtain, then, 2.06 MHz and 3.3 Å for A_{iso} and r_{eff} for the Cu^{II}(TMPA)(1-methylimidazole) complex in spectral simulations at six magnetic fields across the EPR absorption (Figure 6).

The angles α, β, γ, θ_N, and ϕ_N were varied in simulated spectra to assess their effect on the determination of A_{iso} and r_{eff}. Varying α, γ, and ϕ_N was found to have a negligible effect. However, a change in both line shape and frequency of the double-quantum transition was observed when θ_N was varied by 10°, or β by 15°. Even the greatest deviation in θ_N and β though, could be offset by adjusting A_{iso} and r_{eff} by 0.05 MHz and 0.1 Å, respectively.

(32) The angle between Cu(II)–N(1) and Cu(II)–N(6) is calculated by assuming the same coordination structure as for Cu(II)(1,2-dimethylimidazole) (Potenza, M. N.; Potenza, J. A.; Schuger, H. J. *Acta Crystallogr.* **1988**, *C44*, 1201).

(33) q_{xx}, q_{yy}, q_{zz} are three principal values of the electric field gradient tensor, with $|q_{zz}| > |q_{yy}| > |q_{xx}|$.

(34) Edmonds, D. T.; Summers, C. P. *J. Magn. Reson.* **1973**, *12*, 134.

(35) Colaneri, M. J.; Potenza, J. A.; Schugar, H. J.; Peisach, J. *J. Am. Chem. Soc.* **1990**, *112*, 9451.

(36) The principal directions of the quadrupole tensor for 1-methylimidazole were used to obtain the Euler angles because 1,2-dimethylimidazole binds to Cu^{II}(TMPA) differently from imidazole, as deduced from the differences in CW EPR spectra of the two complexes (Figure 2 and Table I).

(37) *Handbook of Organic Chemistry*; Dean, J. A., Eds.; McGraw-Hill, Inc.: New York, 1987; pp 4-45–4-85.

Table III. Electron–Nuclear Coupling Constants for Cu^{II}(dien)(substituted imidazole) Complexes

complex	A_{iso} (MHz)[a]	r_{eff} (Å)[a]	A_{iso} (MHz)[b]	r_{eff} (Å)[b]	e^2qQ (MHz)	η
Cu^{II}(dien)(imid)	1.55	2.9	1.65	3.2	1.43	0.94
Cu^{II}(dien)(1-CH_3-imid)	1.92	3.5	1.80	3.5	2.06	0.20
Cu^{II}(dien)(4-CH_3-imid)	1.54	3.0	1.60	3.2	1.60	0.75
Cu^{II}(dien)(2-CH_3-imid)	1.80	3.3	1.75	3.2	1.73	0.64
Cu^{II}(dien)(1,2-$(CH_3)_2$-imid)	2.20	4.1	2.00	3.5	2.33	0.11

[a] The electron–nuclear coupling constants obtained by spectral simulation at only a single magnetic field near $g_\perp$.[7] [b] The electron–nuclear coupling constants obtained by field-dependent ESEEM simulations at six magnetic fields.

Therefore, these values are taken as the maximum error due to ambiguities in values for α, β, γ, θ_N, and ϕ_N.

The same quality fits of spectra were obtained for other substituted imidazole complexes as well, and the values of A_{iso} and r_{eff} are collected in Table II.

Re-Examination of the Electron–Nuclear Hyperfine Parameters of $d_{x^2-y^2}$ Ground State Complexes. It had been noted by Goldfarb et al.[5] that ESEEM spectral simulations for $d_{x^2-y^2}$ ground state Cu(II)–imidazole complexes carried out at only a single field near $g_\perp$ are inadequate to accurately determine hyperfine parameters. In order to compare the parameters of Cu(II)–substituted imidazole d_{z^2} complexes, as described in this paper, with those of $d_{x^2-y^2}$ ground state complexes, a field-dependent ESEEM study was used to re-examine the electron–nuclear interaction for $d_{x^2-y^2}$ ground state Cu^{II}(dien)(substituted imidazole) complexes.[7]

On the basis of the line shape of the EPR spectrum, the metal ion of Cu^{II}(dien)(1-methylimidazole) is believed to have an elongated octahedral coordination geometry.[12] Three amine nitrogens from the dien moiety and the imino nitrogen from the imidazole roughly form an equatorial plane; g_z is perpendicular to this plane, while g_x and g_y can be along any direction within the plane.[7] The principal directions of the ^{14}N quadrupole tensor of the remote nitrogen of 1-methylimidazole are taken to be the same as in the d_{z^2} ground state complex. If the 1-methylimidazole is coplanar with the equatorial plane, θ_N is 90° and β is 0° (Figure 5b). If, on the other hand, the imidazole plane is perpendicular to the equatorial plane, θ_N is about 80° (90° − 9.3°) and β is 90°. Depending on the orientation of the imidazole plane, θ_N can take any value between 80 and 90° and β, any value between 0 and 90°. If the 1-methylimidazole molecule cannot rotate along the Cu–N(4) bond (Figure 5b), it would have a unique orientation relative to the Cu(II) equatorial plane. If, in contrast, it can freely rotate, the imidazole plane would assume many different orientations and the ESEEM spectrum obtained would be a composite of many spectra, each representing different quadrupole tensor orientations.

In order to test these two possibilities, the value of θ_N was initially varied by 15° to check its effect on simulated spectra. At all six magnetic fields for which data were collected, the shape of the double-quantum line varied slightly, but altering θ_N did not improve the overall fit. Therefore, θ_N was fixed at 90° in the simulation. When β was varied from 0 to 90°, significant changes in the line shape and the intensity of the double-quantum line relative to those of quadrupole lines were observed. With β close to 0°, the line shape and the frequency of the double-quantum line fit the data well at all six magnetic fields, but the intensity of the double-quantum line relative to that of the quadrupole lines was low as compared to the experimental spectrum at the lowest magnetic field setting. In contrast, when β was set to 90°, the fit of the relative intensity of the double-quantum line was better at the lowest magnetic field setting, but the fit for spectra at the high magnetic field settings was not as good. We conclude that simulation with a unique β value is inappropriate and that the experimental data may represent a spectral composite arising from many complexes with the imidazole plane at different orientations relative to the Cu(II)–dien plane. This is consistent with the view that imidazole is able to freely rotate along the Cu(II)–N bond and that the sample used for spectroscopic investigation freezes with heterogeneous imidazole orientations. However, considering the overall fit for spectra at all six magnetic field settings, the values obtained for A_{iso} and r_{eff} are as good as those from simulation using a single β value.

With 0°, 0°, 0° for α, β, γ and 90°, 0° for θ_N, ϕ_N, values of 1.80 MHz and 3.5 Å for A_{iso} and r_{eff}, respectively, gave the best fit for all six spectra of the Cu^{II}(dien)(1-methylimidazole) complex. The electron-nuclear coupling constants obtained by the field-dependent ESEEM simulations at six magnetic fields for three other substituted imidazoles as well as for imidazole, together with those obtained previously by spectral simulation at a magnetic field near $g_\perp$,[7] are given in Table III.

Among all the complexes studied, those with imidazole and 1,2-dimethylimidazole have the largest discrepancy in r_{eff} between values obtained by the two different simulation methods, with the value for imidazole overestimated and that for 1,2-dimethylimidazole underestimated from the value obtained at $g_\perp$ alone. A major factor in determining r_{eff} at only one field near $g_\perp$ is the line width of the double-quantum transition.[7] Because the line width is greatly affected by β, a large error can be introduced without taking into account the structural averaging due to the rotation of the imidazole along the Cu(II)–N(1) bond. For Cu^{II}(dien)(imidazole), although a good fit can be obtained for the spectrum collected near $g_\perp$ by using the parameters determined previously,[7] the dipole interaction for an r_{eff} of 2.9 Å gave too large an anisotropy in the electron–nuclear interaction. As a result, the double-quantum line has a frequency 0.2 MHz lower in the simulation as compared to the experimental data collected at the lowest magnetic field. An r_{eff} value of 3.2 Å is therefore needed to give the appropriate anisotropy. Although the fitting of the line shape is not optimal in the spectrum near $g_\perp$, the best overall fit is obtained for the double-quantum line in all six spectra.

Geometric Effect. The isotropic coupling between the Cu(II) unpaired electron and the remote nitrogen of coordinated imidazole in the d_{z^2} ground state Cu^{II}(TMPA) complex is about 10% larger than that for the $d_{x^2-y^2}$ ground state Cu_{II}(dien)(imidazole) complex (Tables II and III). The anisotropic coupling, as determined by r_{eff}, is somewhat shorter, which suggests that there is more unpaired electron density at the remote nitrogen nucleus in the d_{z^2} ground state complex than in the $d_{x^2-y^2}$ ground state complex.

In octahedral coordinated metal sites, both d_{z^2} and $d_{x^2-y^2}$ orbitals have lobes lying along the metal–ligand bond direction so that they form σ bonds with the ligand orbitals. When the unpaired electron from Cu(II) resides in the d_{z^2} orbital, it is distributed to two lobes along the z axis, which form two σ bonds, and a torus in the xy plane. On the other hand, when the unpaired electron residues in $d_{x^2-y^2}$ orbitals, it is distributed in four lobes along the x and y axes, which form four σ bonds. Therefore, more unpaired electron density is expected to be present in each lobe of a d_{z^2} orbital for a d_{z^2} ground state than in each lobe of a $d_{x^2-y^2}$ orbital in a $d_{x^2-y^2}$ ground state complex. By delocalization through the σ bond formed between one lobe of the Cu(II) ground state orbital and an sp^2 orbital of the directly coordinating imino nitrogen of imidazole, more electron density would reside in the imidazole π system and, thus, in the remote nitrogen nucleus of d_{z^2} ground state complexes. A larger value for A_{iso} and a smaller value for r_{eff}, as found, are therefore reasonable.

An increase of A_{iso} is also seen for 1-methylimidazole and 4-methylimidazole coordinated to Cu^{II}(TMPA) as compared to the case of Cu^{II}(dien) (Tables II and III). However, no increase is seen for 2-methyl- or 1,2-dimethylimidazole. The increase of A_{iso} when imidazole or 1-methylimidazole is replaced by 2-methylimidazole or 1,2-dimethylimidazole in the Cu^{II}(dien) complex is not observed in the Cu^{II}(TMPA) complex. On the contrary, a decrease is observed. A larger copper hyperfine coupling constant, which arises from the interaction between the copper nucleus and the copper unpaired electron, was noted, as compared to that for the imidazole complex (Table I). This suggests that the unpaired electron is less delocalized away from the copper onto the imidazole ring when there is a methyl group at the C(2) position. Therefore, a smaller isotropic component of the electron–nuclear coupling, which is determined by the electron density of the unpaired electron at the remote nitrogen, would be expected (Table II). Both the Cu(II) nuclear hyperfine and the ligand ^{14}N electron–nuclear hyperfine couplings indicate that the Cu(II)–N(5) bond is weaker for 2-methylimidazole, as compared to imidazole, as the axial ligand. This is consistent with the requirement of a 100-fold molar excess of 2-methylimidazole to complex Cu^{II}(TMPA) in H_2O, as compared to less than a 4-fold molar excess of imidazole, although 2-methylimidazole is a stronger base. This weaker binding and smaller electron–nuclear coupling for 2-methylimidazole are attributed to the steric interference caused by the methyl group at the C(2) position.

Such a steric interference is clearly demonstrated by computer modeling. On the basis of the crystal structure of $[Cu^{II}(TMPA)(Cl)]^+$ (Figure 1), three hydrogen atoms attached to the carbons adjacent to the coordinated pyridyl nitrogens of TMPA point toward the C_3 axis. When imidazole binds, it cannot freely rotate along the Cu–N(5) bond due to steric interference from these hydrogen atoms. For 2-methylimidazole, if bound to Cu^{II}(TMPA) with a normal 2.0-Å Cu(II)–N bond length, an additional tilt away from the Cu(II)–N(1) direction is required to prevent collision of the bulky methyl group at C(2) with the pyridyl α-hydrogen atoms. Thus maximal overlap of the Cu(II) d_{z^2} orbital and the ^{14}N lone-pair orbital of 2-methylimidazole cannot be achieved. The delocalization of the Cu(II) unpaired electron onto the imidazole ring π system is suppressed, and the coupling between the unpaired electron and the remote nitrogen nucleus is reduced. Therefore, for Cu^{II}(TMPA) complexes with imidazole substituted at the C(2) position, steric interference alters the electron–nuclear coupling as well as ligand affinity (Tables I and II).

The quadrupole parameters for imidazole complexed to Cu^{II}(TMPA) are almost the same as those for Cu^{II}(dien), with only a slight decrease of both e^2qQ and η (Table II). A similar trend is seen with 1-methylimidazole and 4-methylimidazole. Therefore, the change of Cu(II) coordination geometry from elongated octahedral to trigonal bipyramidal, leading to a change of electronic structure from a $d_{x^2-y^2}$ ground state to a d_{z2} ground state, has little effect on e^2qQ and η. Much more pronounced changes, however, are observed for 2-methylimidazole and 1,2-dimethylimidazole, and this is attributed to unusual binding arising from the steric interference alluded to above.

Solvent Effects. An earlier study of $d_{x^2-y^2}$ ground state Cu(II) complexes showed that an increase in the asymmetry parameter η could be related to a more polarized N–H bond for imidazole than for either 2-methylimidazole or 4-methylimidazole.[7] Alternatively N–H bond polarization could be altered by changing its local environment. The same phenomenon is observed for the d_{z^2} ground state Cu(II) complexes studied here.

No difference was observed in the CW EPR spectrum of Cu^{II}(TMPA)(substituted imidazole) complexes whether prepared in acetone or in H_2O. Therefore, one might conclude that solvent has no discernible effect on the structure of the Cu(II) site and its immediate ligands. Differences, however, are observed in the quadrupole parameters, and these are attributed to the effect of solvent on the remote nitrogen of the coordinated substituted imidazoles. Since acetone has a higher dipole moment than H_2O, it is expected to form a stronger hydrogen bond and thus polarize the N–H bond to a greater extent. The EFG along the N–H bond is increased in acetone, leading to an increase of the asymmetry parameter η and a decrease of the nuclear quadrupole coupling constant e^2qQ, as seen for the 4-methylimidazole and 2-methylimidazole complexes.

A decrease of the asymmetry parameter η is seen, though, for the imidazole complex in acetone as compared to water. As shown for $d_{x^2-y^2}$ ground state complexes,[7] the direction with the largest value of the EFG, q_z, is perpendicular to the imidazole plane for all the substituted imidazoles, with η much smaller than unity. The second largest electric field gradient is along the N–H bond. An increase of N–H bond polarization results in an increase of the electron field gradient along the N–H bond and this leads to an increase of η. A switch of q_z from the direction perpendicular to the imidazole plane to in-plane and along the N–H bond direction occurs when the EFG's along these two directions become equal and η approaches unity. A further increase of N–H bond polarization results in a decrease of η away from unity.

The EFG along the N–H bond direction for imidazole coordinated to Cu^{II}(TMPA) is nearly the same as or even larger than that perpendicular to the imidazole plane. The increase of the N–H bond polarization caused by acetone increases the EFG along the N–H bond further so that its magnitude is greater than that in the direction perpendicular to the imidazole plane. As a consequence, the greater N–H bond polarization is accompanied by a decrease rather than an increase of η away from unity.

Conclusion. In d_{z^2} ground state Cu(II) complexes, it is the remote nitrogen of axially coordinated imidazole that gives rise to spin echo modulations. Changing the electronic structure of Cu(II) from a $d_{x^2-y^2}$ to a d_{z^2} ground state slightly increases the electron–nuclear coupling for the remote nitrogen of coordinated imidazole, while the ^{14}N nuclear quadrupole interaction is almost unaffected.

Acknowledgment. This work was supported by USPHS Grants GM 40168 and RR 02583 to J.P. and GM 28962 to K.D.K. F.J. would like to thank J. W. Sam for editing this manuscript.